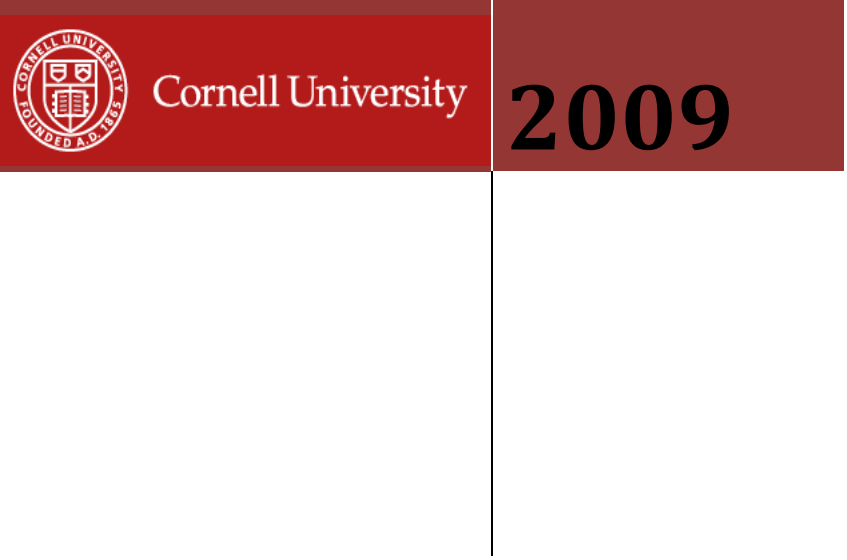

Biodegradable Implant with TGF-β Delivery for Enhanced Healing of Bone Tissue: A Computational Model

BEE 4530: Computer-Aided Engineering: Biomedical Processes

Professor Ashim Datta

Group 4: Kevin Eckes, David Post, Bryan Sutermaster, Sarah Villarreal

Table of Contents

Executive Summary

In most common fractures, bone is able to heal itself over a six week time period. Catastrophic fractures, however, may require that shards of bone be removed surgically, leaving critical size defects in fracture areas that are unable to heal in a reasonable amount of time. For this reason, bone is frequently targeted by tissue engineering and drug delivery strategies aiming to encourage bone regeneration. Often, such strategies involve scaffolds or implants in combination with cells and/or growth factors. One major design requirement in growth factor delivery from such an implant is that it must exhibit controlled growth factor release, defined by relatively constant flux over time. Additionally, the growth factor must remain in the tissue at an effective concentration over the time required for healing. We report on a computational model and analysis of the release of Transforming Growth Factor β (TGF-β) from a spherical, collagen-based implant with biodegradable polymer-coated layers containing varying concentrations of TGF-β. This model, created using COMSOL Multiphysics software, allows for rational design of a biodegradable, drug-eluting implant for tissue regeneration. Using such a model, it is easily possible to simulate a variety of conditions (such as different numbers of layers or different initial concentrations of drug within each layer) in order to achieve relatively constant flux and sustain a physiologically effective concentration of the growth factor over time. The following simulations were run: non-layered construct with uniform growth factor concentration throughout; five-layered sphere with radially increasing concentrations; five-layered sphere with radially decreasing concentrations; ten-layered sphere with radially increasing concentrations; ten-layered sphere with uniform concentration; ten-layered sphere with radially decreasing concentrations. We observed that spheres with more layers exhibited a quasi-linear drug release profile, and that radially increasing initial growth factor concentration in the layers, such that the highest concentration is at the center, results in relatively constant flux. We also show that over time, an implant with radially increasing initial TGF-β concentration exhibits sustained release within the range of the effective concentration of TGF-β in hyaline cartilage. Our model is important because it can be used to design drug delivery devices rationally before costly and time-consuming wet-lab experiments are done. Furthermore, our model can be extended to a variety of other drug delivery situations which require construct degradation coupled with controlled release.

Introduction and Design Objectives

Although bone has a natural capacity for bone regeneration and growth, events such as bone fractures, bone malformation, cancer, or reconstructive cosmetic surgery require aided bone generation. Taking bone fractures in particular, 50% of Americans 50 years of age or older are at risk for fracture due to osteoporosis or low bone density. Bone fractures result in about 6.8 million doctors' visits each year, costing $30 million dollars a day in the United States alone. Therefore quick, simple, and low-cost methods to aid the

healing process are of increasing interest for health care professionals and researchers alike.

One method to encourage bone generation is implant technology that stimulates surrounding bone growth onto an inserted matrix/scaffold. Tissue-engineering techniques have been successful in bone and cartilage regenerative repair due to the relatively low vascularization, and thus infrequent elicitation of an immune response. One of the most promising implants proposed for bone generation was by Gombotz et al. (1993) who used a polymer/DBM (demineralized bone matrix) biodegradable gel. The gel could be injected into sights of injury with or without the aid of a biocompatible metal rod to aid the bone healing process. As the polymer of the gel degraded, it left a cartilage matrix that was slowly replaced by naturally growing bone during healing.

The gel was composed of 30% weight/volume poly(lactic-co-glycolic-acid), or PLGA, and a DBM containing TGF-β. PLGA was used based on its biodegradation rate, biocompatibility, mechanical properties, and pharmacokinetic release properties (Gombotz 1993). Transforming Growth Factor-β, TGF-β, is a 25-kD globular protein that has been shown in several studies to stimulate osteoblast and osteoclast activity and to successfully increase bone growth (Amento 1993). Demineralized bone matrix has also been shown to induce cartilage growth and osseous reconstruction (Glowaki 2009).

For our project we decided to create a computer model that simulated the biodegradation and drug release from an implant somewhat similar to that described by Gombotz et al. for bone repair. The model encompasses the implant's interactions with the surrounding tissue of cartilage and bone and is run over the entire time required for bone healing.

Our computational model examined the ability of the biodegradable implant to administer an effective concentration of TGF-β at a steady rate to a bone fracture site for an extended period of time. In order to achieve steady release of growth factor, it is necessary to have quasi-constant flux of TGF-β out of the implant. Because of this condition, our model differs from the implant described by Gombotz et al. Instead of the implant being composed of a PLGA/DBM gel with a homogenous concentration of TGF-β, our implant is composed of a multi-layered implant, in which collagen gel layers are entrapped between thin membranes of plastic (non-gel form) PLGA. We chose to model the layers as collagen gel instead of DBM for several reasons. Collagen gel has the same effect on bone healing and has been shown to induce natural cartilage growth and bone reconstruction like DBM (Glowacki, 2009). Additionally, in order to model biodegradation of the implant, the gel must be composed of a material with similar or the same properties as the injury site during early healing stages. During the reparative phase of bone healing the injury site is filled with hyaline cartilage, which is later mineralized to form bone (Glowacki, 2009). Since cartilage is in large part composed of collagen, we chose collagen as our TGF-β-containing layer material.

Between each membrane is a composition of collagen gel with a specific initial concentration of TGF-β. Each layer is uniform (in thickness, collagen content, etc), but concentration of TGF-β in the collagen is varied. Thin membranes of plastic PLGA covering each collagen layer keep the TGF-β from diffusing into the rest of the implant, thereby maintaining the initial concentrations of TGF-β in each layer. During implant degradation, the PLGA layer comes in contact with the physiological environment of the implant and degrades, thereby releasing TGF-β into the injury site from the collagen layer beneath. We modeled the dissolution time of each plastic PLGA membrane using a literature-based equation for the biodegradation of a solid PLGA sphere with a diameter of 6 mm.

During implant biodegradation, the collagen gel composite releases TGF-β into the surrounding tissue. The initial concentration of TGF-β in each layer of the sphere was defined based on a gradient varying from 0.1 mg/ml to 1 mg/ml to obtain quasi-constant flux of the therapeutic TGF-β out of the implant. Furthermore, this range encompasses the effective dose needed in the implant for maintained therapeutic properties. We modeled the implant inserted into a complete fracture in a human femur that typically takes 6-9 weeks to heal, but we wanted to show that TGF-β release could be sustained for the time needed for the entire implant to degrade. According to the PLGA degradation equation, it would take our implant 92.5 days to degrade completely, so we programmed COMSOL to simulate a 92.5-day period.

With this model we aimed to:

- Determine the optimal initial drug concentration profile within the biodegradable implant for quasi-constant flux of drug
- Computationally model implant biodegradation in order to achieve sustained drug delivery well over the time needed for bone repair
- Ascertain whether or not our design maintains an effective concentration of drug in the tissue for a sufficient period of time to induce replacement of the hyaline cartilage with bone.

Model Design

In order to evaluate the behavior of this biodegradable implant and the drug delivery profile, we used COMSOL Multiphysics to generate a simulation of the implant degradation and drug release over the time of *in vivo* bone healing in a typical adult human femur. The implant was modeled as a sphere with surrounding hyaline cartilage according to the typical healing process of bone. The cartilage was modeled as 2.4 cm thick, according to the typical size of an incomplete critical size fracture in a human long bone. Surrounding the cartilage on the top and bottom was bone to simulate implantation into the bone break. The bone layer was modeled as 0.6 cm thick based on what we determined to be a reasonable computational domain. The geometry and size of the

implant modeled was chosen after review of the Gombotz patent for this therapy, and other related implants for bone repair (Gombotz 1993, King 2001). The spherical geometry of the implant and axisymmetry of a human long bone allowed us to use a two-dimensional axisymmetric model to reduce our simulation's computation. The geometry and dimensions of the computational domain are shown in Figure 1 below.

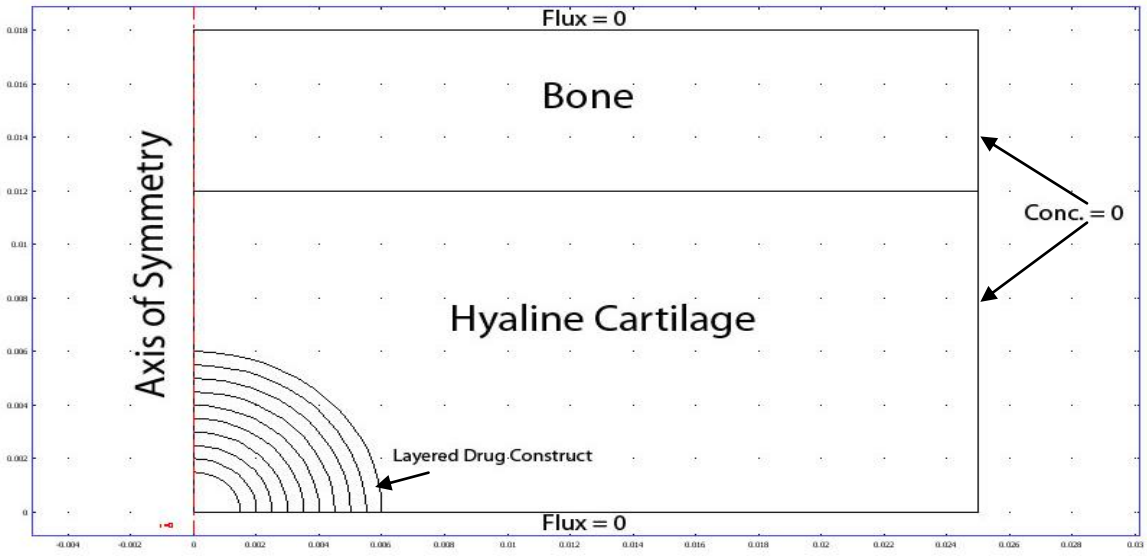

Figure 1. Schematic of computational domain for COMSOL model.

The governing equation for our analysis is:

$$\frac{\partial C_a}{\partial t} = D_{ab}\left(\frac{1}{r}\frac{\partial}{\partial r}\left(r\frac{\partial C_a}{\partial r}\right) + \frac{\partial^2 C_a}{\partial z^2}\right)$$

Note that there is no need to consider convection, due to the relative lack of fluid flow in this area of the body. Also, since our therapeutic agent is a peptide hormone, it is not expected to experience a significant rate of degradation in the tissue, allowing the reaction term to be ignored. The left boundary, as indicated, is the axis about which our model is axi-symmetric. The model is symmetric about the bottom boundary and thus is set to a zero-flux condition. The top boundary is also set to zero flux conditions, as a negligible amount of drug diffuses that far into the tissue over the time period of our computations. The right boundary condition is a zero concentration boundary condition because we assume that blood vessels near the injury site will rapidly remove all TGF-β that diffuses that far away from the implant. Initial conditions include the concentrations of drug in each layer of the implant, which will be adjusted accordingly throughout our

project in order to determine an arrangement that provides a relatively constant rate of flux. Furthermore, the concentration of TGF-β in the bone and cartilage tissue is assumed to be zero initially.

The simulation was run over 92.5 days with a time step of 12 hours. The simulation time is based on the average time for complete bone repair of an average fracture, along with the time it would take for an implant of 6 mm to degrade. We based our choice of a 12-hour time step on the effective diffusion of TGF-β and computer computational constraints. The time step was constant throughout the simulation to capture the effects of the changing implant diameter and amount of drug diffusing from each subsequent layer. We used an unstructured mesh with finer mesh closer to the drug sphere due to dynamic changes expected near this area.

The diffusivity of TGF-β in hyaline cartilage was modeled as $40x10^{-12}m^2/s$, and in bone as $1x10^{-6}$ m^2/s, based on literature values for diffusivity values of proteins and molecules of similar size in each tissue (Leddy 2003, Nauman 2007, Williams 2007). A reaction term was not included in the governing equation since TGF-β is a ligand that binds to cell surface receptors without internalization. Therefore *in vivo* concentrations can be modeled as unaffected by cellular uptake.

In order to simulate the biodegradation of the implant, the disc was modeled with either five or ten layers that dissolved according to the degradation rate of a solid PLGA sphere. To simplify the model enough to implement it, we had to assume the entire implant was made of PLGA in order to calculate the degradation time of each thin PLGA layer. A macro was then programmed to "dissolve" each layer at a specific time determined by the biodegradation rate of the polymer PLGA. This was actually done by using the macro to change the diffusivity of TGF-β in each collagen layer from zero to $40x10^{-12}$ m^2/s when the neighboring PLGA layer degrades. Therefore, our model is also based on the assumption that no TGF-β diffuses through the PLGA layer until it has been completely degraded.

Since literature values for the biodegradation of our collagen-PLGA layered sphere are unavailable, the degradation rate of the polymer was used. This simplification is fairly realistic since only the thin polymer layers degrade, leaving behind collagen matrix that is replaced by natural hyaline cartilage in the normal bone healing process. The biodegradation rate of 50:50 PLGA (50% poly(lactic acid), 50% poly(glycolic acid)) *in vivo* was determined by using the half-life of this polymer from literature along with the following equation:

$$N_t = N_0 e^{-\lambda t} \quad (1)$$

where N_0 is the initial mass of the spherical implant, N_t is the quantity that still remains and has not yet decayed after a time t, and λ is a positive number called the decay constant of PLGA. Using the known radius of each layer, the volume of the sphere,

and the absolute density of PLGA, the time each layer dissolves was determined. For detailed calculations see Appendix D.

Each layer had a different concentration of the TGF-β in order to maintain a semi-constant flux out of the implant over time and over the change in geometry as the sphere shrinks. The initial concentration in each layer of the sphere was defined based on a gradient varying from 0.1 mg/ml to 1 mg/ml. As the volume of the sphere shrinks, the space will be filled with a collagen gel/matrix according to the natural healing process of bone. Therefore the implant's geometry and drug concentration will vary with time, causing a time step change in the tissue/implant interface.

Results and Discussion

Because the diffusivity values we obtained were not obtained under the same experimental conditions we are working with, we conducted a sensitivity analysis to determine how much this might affect our results. To measure the sensitivity of computation to the diffusivity parameters we used, we used post-processing integration to determine the average concentration of TGF-β in the cartilage matrix after varying bone and cartilage diffusivity by -20, -10, 0, 10, and 20 percent. Figure 2 below depicts the effect of diffusivity values in both bone and cartilage on the average concentration values. Clearly, the model is more sensitive to changes in TGF-β's diffusivity in cartilage. For the diffusivity of TGF-β in bone, there is only slight variation.

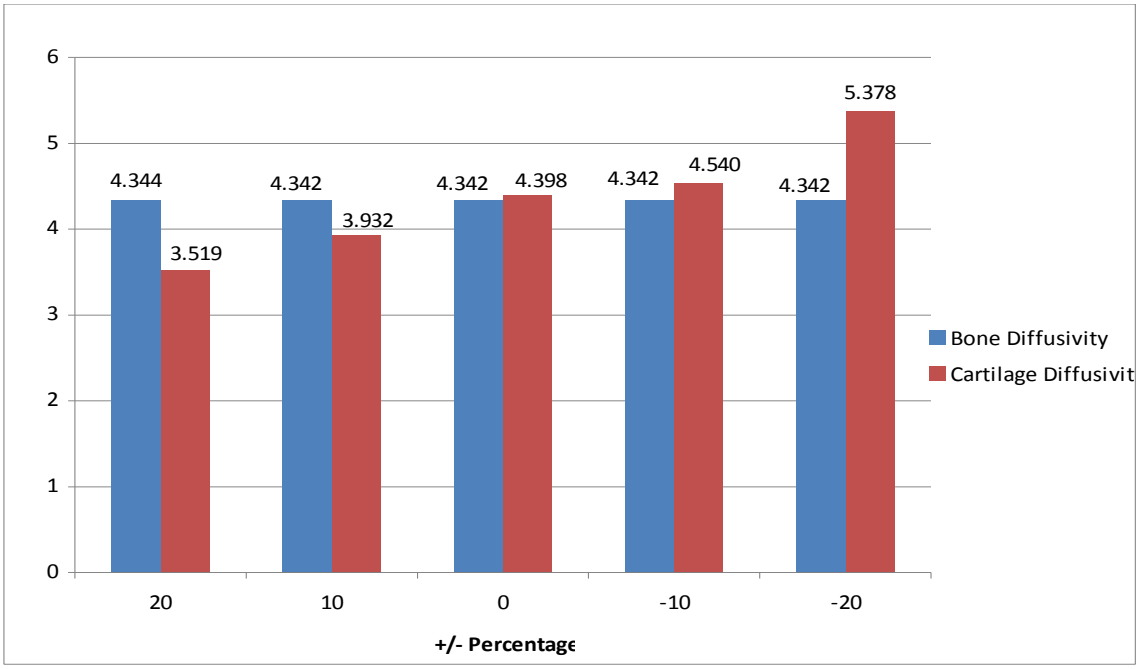

Figure 2. Sensitivity of computational model to changes in diffusivity of TGF-β in bone and cartilage regions.

Next, we analyzed our model by varying the number of layers and the initial TGF-β concentration in each layer in order to determine which arrangement provided the most constant flux over time. For comparison against our layered spherical implant, we used a classic drug-eluting sphere, which was un-layered and loaded with a uniform concentration of TGF-beta (black curve in all figures). For our layered model, we tested which was most effective: increasing drug concentration from inside to out, maintaining a constant drug concentration throughout, or decreasing drug concentration from inside to out. Figure 3 illustrates the results of these trials. The homogeneous model releases its drug rapidly and in an uncontrolled manner. While all layered models out-perform the homogeneous model, the most constant flux of drug results when concentration decreases linearly from the inside of the scaffold to the outside. It is also interesting to note that even with constant concentration of drug throughout, our layered implant releases drug in a far more controlled manner than traditional methods.

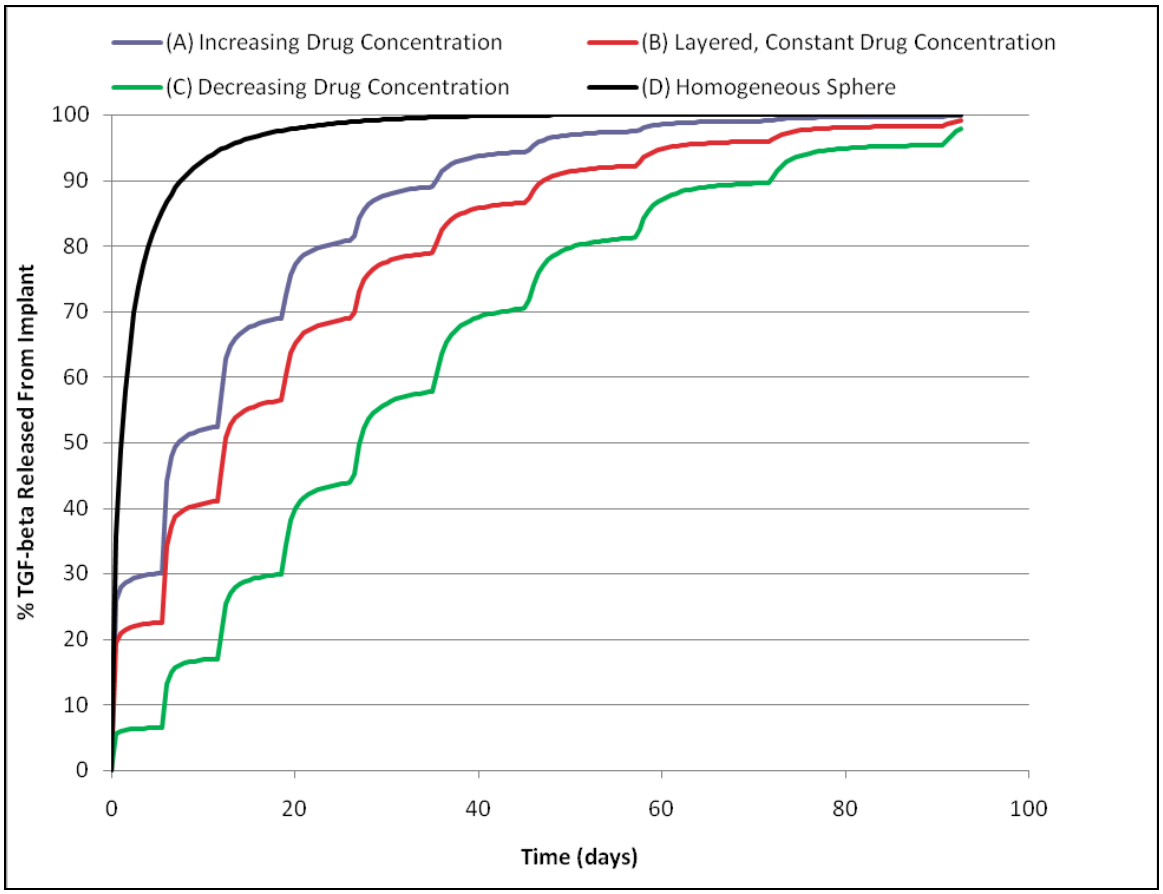

Figure 3. Percentage of the total TGF-beta initially in the implant that has been released versus time. (A) Represents the case where TGF-beta concentration linearly increases as one moves from the inside of the sphere to the outside. (B) Represents the case where TGF-beta concentration remains constant throughout the sphere, but layers are still present and separated by impermeable membranes. (C) Represents the case where TGF-beta concentration linearly decreases as one moves from the center of the sphere to the outside. (D) Represents the case where there are no internal boundaries, i.e. a homogeneous sphere filled with a constant concentration of TGF-beta.

Furthermore, we hypothesized that increasing the number of layers would further control TGF-β release, and the stair-stepping observed in Figure 3 would approach a more linear release. Figure 4 shows the difference in drug release between the increasing concentration and decreasing concentration models with both five layers and ten layers. One can see that as we double the number of layers, drug release becomes more controlled and more linear in nature.

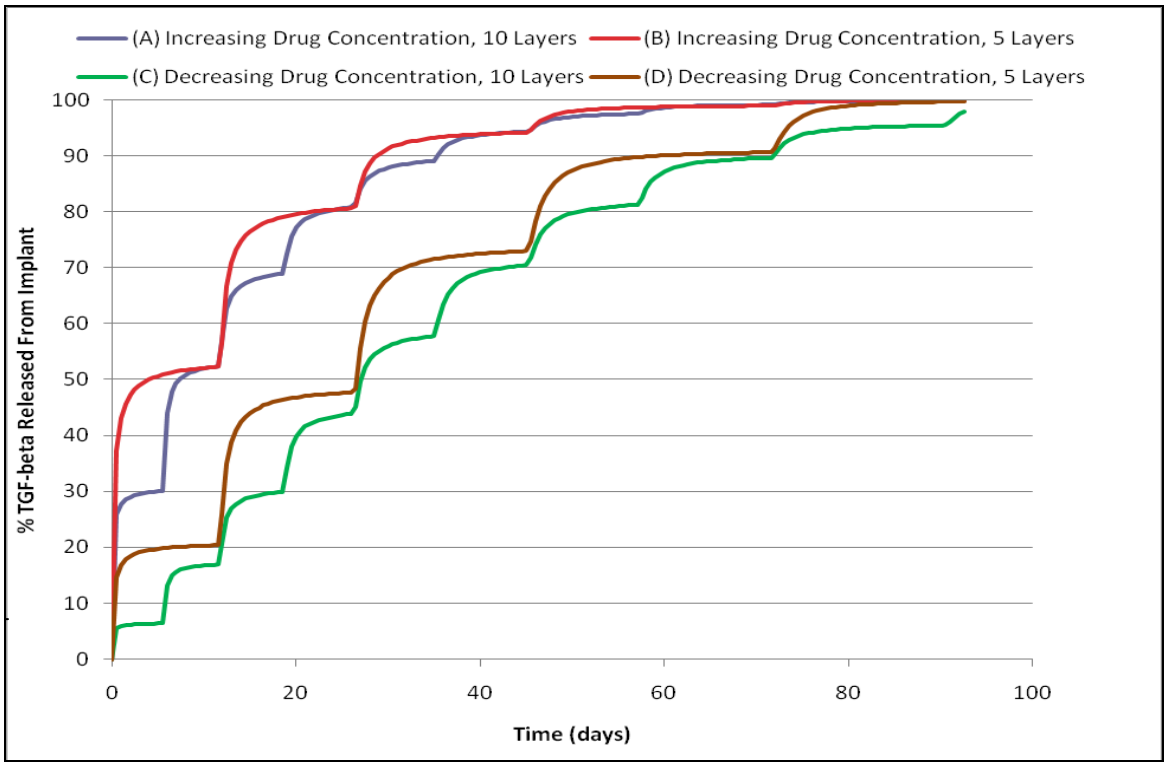

Figure 4. Percentage of initial scaffold TGF-beta eluted versus time for (A) a ten-layer implant model with increasing concentration from the center to the outside of the sphere, (B) a five-layer implant model, also set up with a linearly increasing concentration from the inside of the implant to the outside, (C) a ten-layer implant model with concentration linearly decreasing from inside to out, and (D) a five-layer implant model with concentration linearly decreasing from inside to out.

Lastly, we sought to determine the effectiveness of this scaffold at delivering our drug into the cartilage, and thus achieving its purpose. Figure 5 shows the concentration of TGF-beta in the cartilage for each of the different models. With the homogenous sphere, one observes that there is a rapid initial increase in drug concentration, but the majority of drug is eliminated from the system within 40 days. However, as one adds membrane-separated layers, the drug release becomes steadier and drug permeates through the cartilage for a longer period of time. Again, the model of drug concentration decreasing from inside to out shows the most sustained cartilage drug concentration, with the concentration varying the least throughout the 80 days. This model also performs such that it sustains release of TGF-β at concentrations very close to the therapeutic range (0.1 µg/ml to 1 µg/ml, as shown by the area between the two horizontal orange lines).

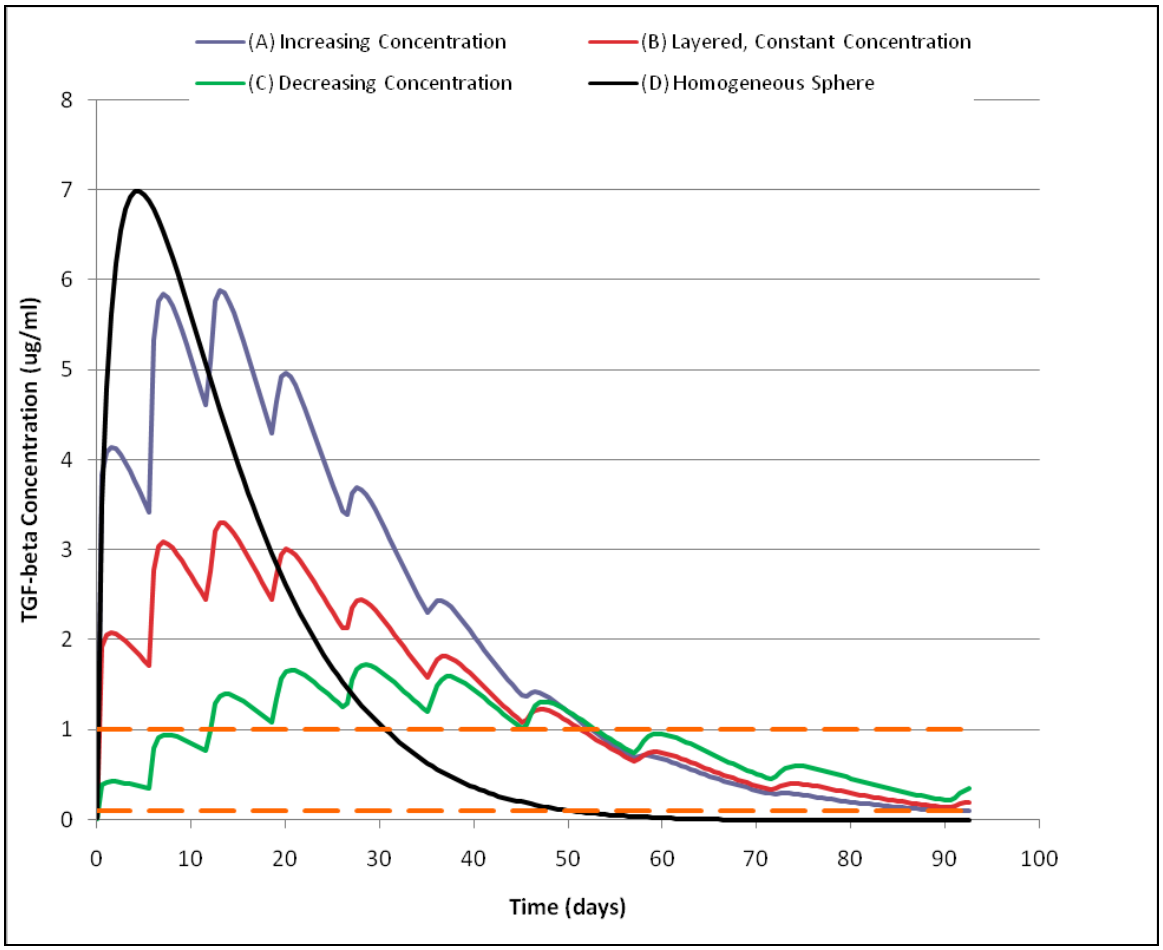

Figure 5. Concentration of TGF-beta in the cartilage as a function of time. (A) represents the situation where initial drug concentration in the sphere increases linearly from inside out, (B) where the concentration is the same throughout, but layer boundaries are still present, (C) where the concentration decreases linearly from the center of the sphere to the surface, and (D) where the sphere has no layers and starts with the same drug concentration throughout. Orange lines depict the therapeutic range of concentrations for TGF-β (0.1 µg/ml to 1 µg/ml).

Lastly, we had to compare our model to known experimental results in order to demonstrate its validity. We compared our results to the results of wet lab experiments (Gombotz et al, 1993) involving the release of TGF-beta from a mixture of DBM and PLGA. These implants were cylindrical—2 mm in diameter and 2 mm thick. 25 µg of TGF-beta and a 40 µl solution of radiolabeled TGF-beta were added to the construct initially. A gamma counter was used to measure the amount of radiolabeled TGF-beta that was released from the scaffold. These results are summarized in the Figure 6 below.

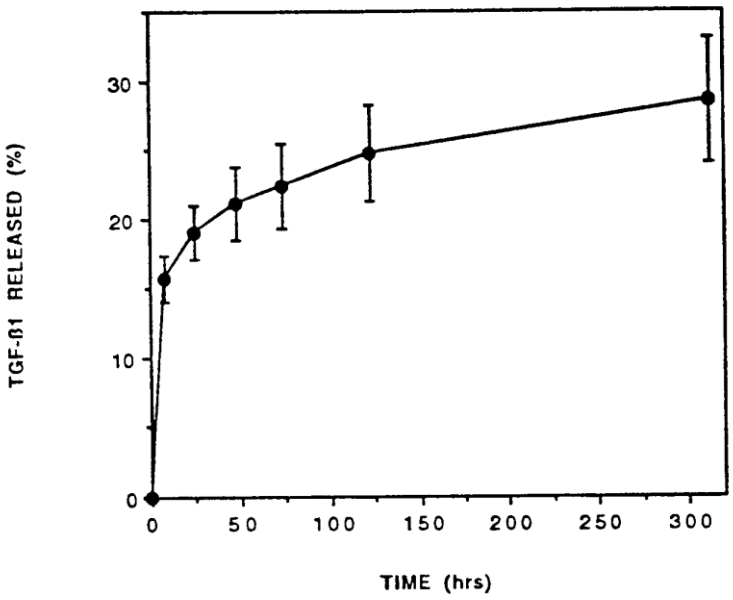

Figure 6. Cumulative amount of TGF-beta released from PLG/DBM device over time (Gombotz et al, 1993)

Our computational results are shown below, in Figure 7. Over similar same time points as chosen in the patent summary, we show that the curve shape and percent of drug released is fairly comparable.

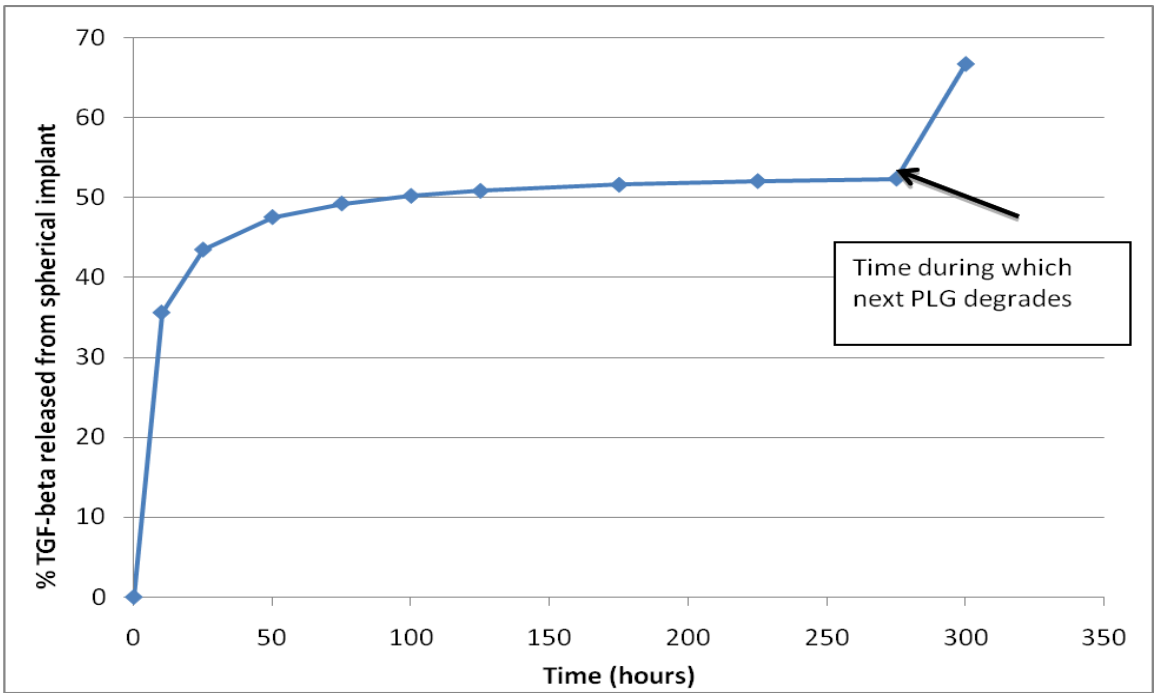

Figure 7. Cumulative amount of TGF-beta released from spherical implant over 300 hours.

Because our drug delivery construct is conceptually very different from the construct in the patent, we did not expect complete correspondence between the patent's reported values and our calculated values. In addition to design differences, we obtained diffusivity values from several other sources, so it is reasonable to see large differences between our computational results and their experimental results. We do, however, show that we obtain a cumulative release curve of similar shape over the same time scale that the patent reports. In Figure 7, the reason for the "jump" at 275 hours is the complete degradation of the first PLGA diffusion barrier, and therefore release of additional TGF-beta.

Conclusion and Design Recommendations

The results of our computational model show that a layered drug implant can deliver TGF-β to a bone injury site in a controlled, linear manner. Furthermore, our model can achieve and sustain physically relevant concentrations of TGF-β in the cartilage subdomain. The layered geometry, when arranged such that the innermost layer is the most concentrated and the outermost layer is the least concentrated, achieves a pseudo-linear release profile over a ninety day period. Conversely, when the outermost layer is the most concentrated and the innermost layer is the least concentrated, the release profile is more hyperbolic, like that of a non layered, homogenous concentration implant. The implant in which concentration decreased from inside to out provided the most constant flux and the most sustained release, and is thus the most desirable for bone healing. Additionally, this implant maintained a therapeutic level for the longest time period in comparison to the other implants.

In the ideal case, there would be a linear concentration gradient of TGF-β such that the highest concentration was contained in the center point of the spherical geometry. However, our model utilizes a finite number of layers, as it is impossible to manufacture an implant with a perfectly continuous TGF-β gradient. In our investigations, the addition of more layers improved the linearity of our TGF-β release profiles. However, because concentrations undergo large and rapid changes at the boundaries between internal layers at their respective release times, additional mesh elements would be required to accurately compute the concentrations in these regions. Such an addition of mesh elements would make the model increasingly computationally intensive. In the future, we would have to weigh the benefits of adding additional layers to get a more continuous profile versus the longer computation time, in order to find the optimal number of layers to model.

Another necessary simplification of the ideal situation is the finite release times of the layers. The approximate mass of each layer and degradation times were calculated and based on a literature-obtained half-life of PLGA. We programmed COMSOL to "degrade" the PLGA membranes stepwise using a macro logic function that changed the diffusivities of TGF-β in the layer from zero to that of TGF-β in collagen at specified release times. In the ideal case, the implant would be degrading and releasing drug continuously. There are two ways that the simplification can be brought closer to the ideal case. First, reducing layer thickness would cause release times to be more frequent,

which more closely approximates the ideal case in which very thin layers would be sloughed off continuously. Second, one could implement a moving mesh and moving internal boundary to model the degradation of the implant. In future studies, both of these alternatives would be explored and compared to the stepwise release approach.

Practical limitations primarily include simplified geometry, estimated diffusivity values, control of manufactured layer thickness, and the idealized biodegradation process. We have simplified the geometry to a great degree, and could adjust the geometry so as to more accurately represent the break. In a medical situation, MRI or CT data could be used to obtain the geometry of a typical fracture. As the precise data for the diffusivities of TGF-β in cartilage and bone are not readily available, we would need to execute an independent experiment to accurately measure these parameters. In the actual manufacturing process, it might be difficult to control the layer thickness over the entire sphere with any great precision. Also, because our product only dealt with an idealized model, we can only recommend a preliminary manufacturing procedure. Finally, the PLGA degradation process used in this study is assumed to be uniform. In reality, the membranes would most likely not degrade uniformly. Rather, the membranes would probably develop pores through which TGF-β could "leak" before the entire membrane degraded completely.

In reality, this implant can be manufactured by a stepwise dip-coating process. First a spherical core of a high weight percent collagen gel can be constructed containing a defined high concentration of TGF-β. After allowed to cure for an appropriate amount of time, a thin plastic layer of PLGA can then be deposited through a similar dip-coating, or possible a spin coating process. This collagen dip-coating, followed by PLGA dip coating procedure would then be repeated with specified TGF-β concentrations until the predetermined number of layers is achieved.

Using COMSOL, we were able to simulate a number of variations of a single drug release model. COMSOL helped us gain fundamental understanding of the physics of drug diffusion from a biodegradable implant. The software allowed us to show, with reasonable certainty, that a layered, biodegradable, drug-eluting implant can achieve quasi-constant flux and maintain an effective drug concentration for the entire time period required for bone healing. In a research environment, a computational model such as ours could act as a stepping-stone between concept and costly, time-consuming wet-lab experiments.

Works Cited

Amento, E.P., Xu, Y., Deguzman, L., Lee, W.P., Nguyen, T., Gillet, N.A. "TGF-beta 1 Induces Bone Closure of Skull Defects." *J Bone Miner Res*, 1993: 753-761.

Anderson, J.M., Matthew, S.S. "Biodegredation and biocompatibility of PLA and PLGA microspheres." *Advanced Drug Delivery Reviews, Vol 28*, 1997: 5-24.

Datta, A., Rakesh, V. *Computer Aided Engineering: Applications to Biomedical Processes.* Ithaca, NY: Cornell University Department of Biological and Environmental Engineering, 2008.

Filvaroff, E., Erlebacher, J, Ye, S.E., Gitelman, J., Lotz, J., Heillman, Derynck, R. "Inhibition of TGF-beta receptor signaling in osteoblasts leads to decreased trabelcular bone mass." *Development, Vol 126*, 1999: 4267-4279.

Glowacki, J., Zhou, S.H., Mizuno, S. "Mechanisms of Osteoinduction/Chondroinduction by Demineralized Bone." *Journal of Craniofacial Surgery, Vol 3*, 2009: 634-638.

Gombotz, W.R., Pankey, S.C., Bouchard, L.S., Ranchalis, J., Puolakkainen, P. "Controlled release of TGF-Beta 1 from a biodegradable matrix for bone regeneration." *J Biomater Sci Polymer Edn, Vol 5(1/2)*, 1993: 49-63.

Gombotz, W. A Biodegradable TGF-beta delivery system for bone regeneration. New York Patent 0567391A1. October 27, 1993.

King, G.N. "The Importance of Drug Delivery to Optimize the Effects of Bone Morphogenetic Proteins During Peridontal Regeneration." *Current Pharmaceutical Biotechnology, Vol 2(2)*, 2001: 131-142.

Leddy, H. & Guilak, F. "Site-Specific Molecular Diffusion in Articular Cartilage Measured using Fluorescence Recovery after Photobleaching." *Annals of Biomedical Engineering, Vol 31*, 2003: 753-760.

Nauman, J., Campbell, P., Lanni, F., Anderson, J. "Diffusion of Insulin-Like Growth Factor-1 and Ribonucleas through Fibrin Gels." *Biophysical Journal, Vol 97*, 2007: 4444-4450.

Williams, R.M., Zipfel, W.R., Tinsley, M.L., Farnum, C.E. "Solute Transport in Growth Plate Cartilage, In Vitro and In Vivo." *Biophysical Journal, Vol 93*, 2007: 1039-1050.

APPENDIX A – Mathematical Statement of the Problem

Schematic:

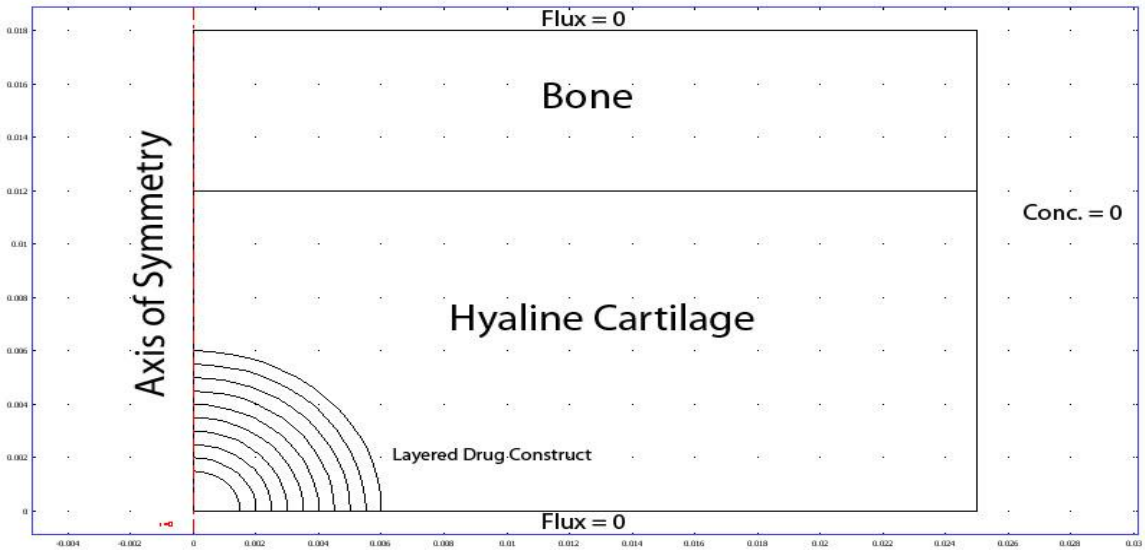

Governing Equation for Mass Transfer – Cylindrical Coordinates

$$\frac{\partial c}{\partial t} = D_{AB}\left(\frac{1}{r}\frac{\partial}{\partial r}\left(r\frac{\partial c}{\partial r}\right)+\frac{\partial^2 c}{\partial z^2}\right)$$

Initial Conditions:

- Five-layered sphere with radially decreasing concentration (1.0, 0.8, 0.6, 0.4, 0.2 mg/ml)
- Five-layered sphere with radially increasing concentration (0.2, 0.4, 0.6, 0.8, 1.0 mg/ml)
- Ten-layered sphere with radially decreasing concentration (1.0, 0.9, 0.8…0.4, 0.2, 0.1 mg/ml)

- Ten-layered sphere with radially increasing concentration (0.1, 0.2, 0.3…0.9, 1.0 mg/ml)
- Ten-layered sphere with uniform concentration (0.5 mg/ml)
- Non-layered sphere with uniform concentration (0.5 mg/ml)

Boundary Conditions:

TOP: Zero flux condition

RIGHT: Zero concentration condition (assume blood carries away growth factor)

BOTTOM: Zero flux condition (due to symmetry)

Appendix B- Mesh Convergence:

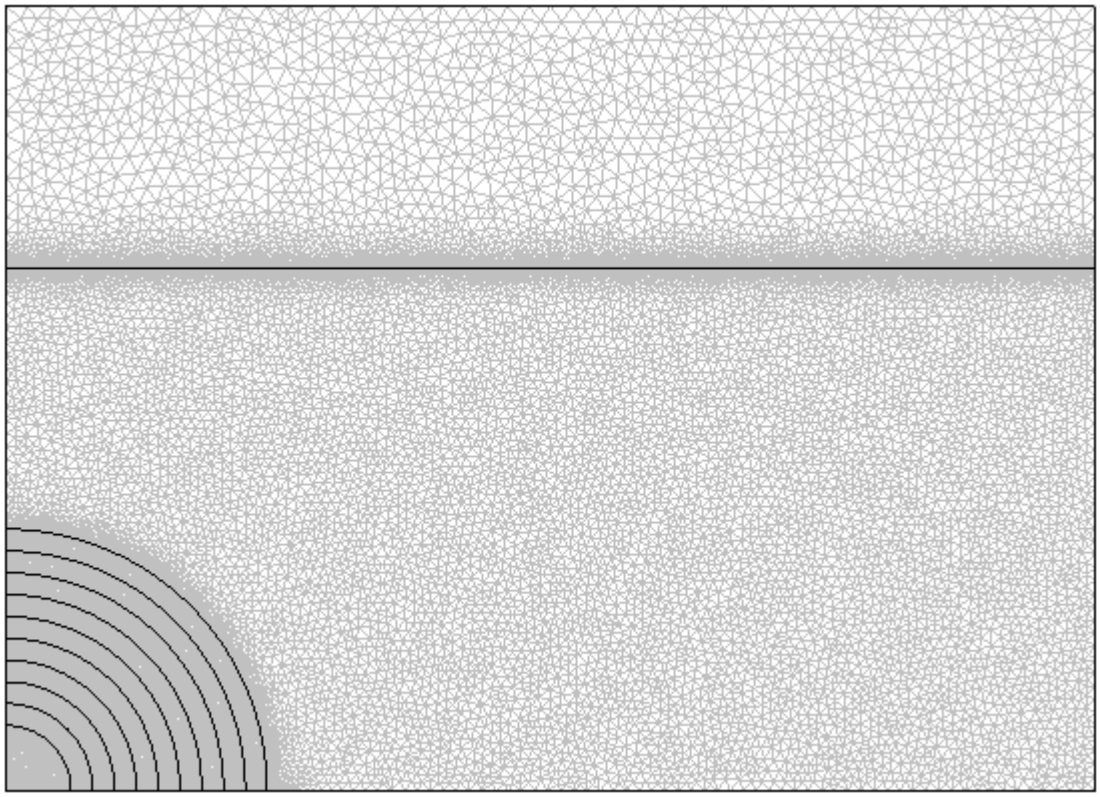

Figure A-B1. Meshed geometry for 10-layer implant case.

Note in Figure A-B1 that the entire implant surface must have very fine mesh since the implant/tissue interface will be a major site of diffusion, and thus extremely important in calculations. These regions should be as non-discretized as possible to capture the physical reality as much as possible. The bone-cartilage interface is also assumed to be very important, and therefore is given an extra number of mesh elements. The bone itself, on the other hand, plays less of a role in TGF-beta diffusion, and thus is given a relatively course mesh.

Next, we performed a mesh convergence analysis to examine whether what extent of meshing was necessary to gain the best balance between simulation accuracy and time required to complete the simulation. As the number of mesh elements increases, the concentration of drug in the cartilage changes as well. However, after a certain point, similar increases in mesh element number provide only marginal increases in accuracy, and can severely add to computation time. As is apparent from the plot, the optimal number of mesh elements is our setup containing 25,175 elements, as there is only a slight change in TGF-beta concentration in the "hyaline cartilage" domain upon remeshing with more elements. Therefore, we used 25,175 elements for our computations.

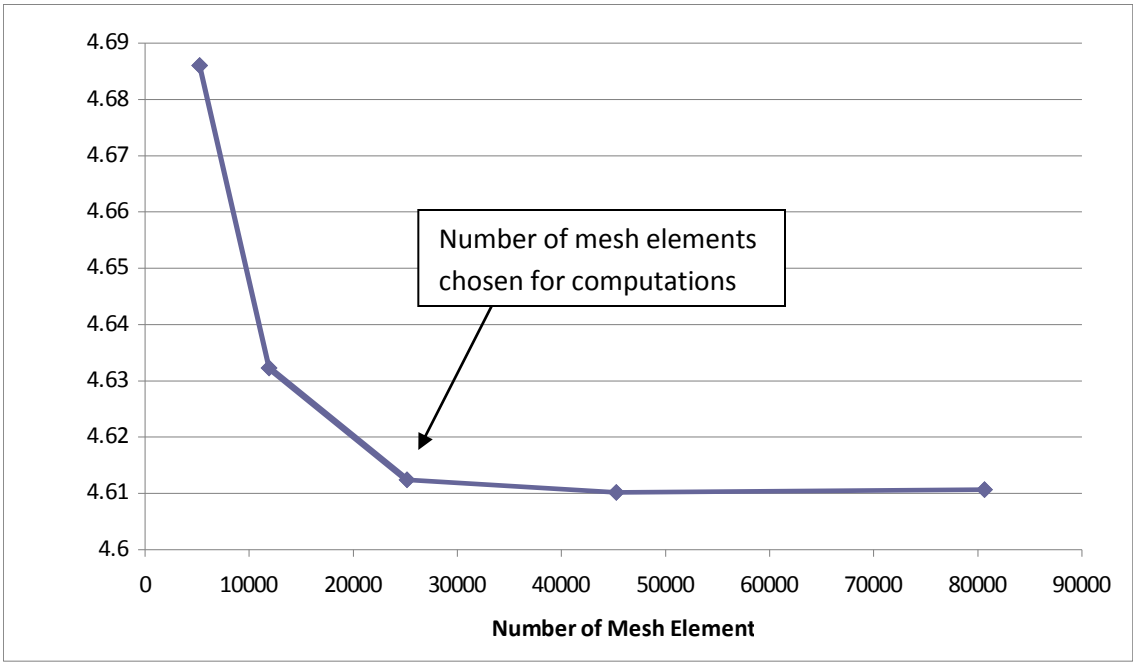

Figure A-B2. Mesh Convergence Analysis – plot of average concentration vs. number of mesh elements.

Appendix C - Property Values:

Property values used in our calculations as well as the sources from which they were obtained are shown below in Table A-C1:

Table A-C1. Property values and their sources.

Property	Value	Units	Source
Cartilage diffusivity	40*40^-12	m^2/s	(Leddy & Guilak, 2003)
Bone diffusivity	1*10^-6	m^2/s	(Nauman, Campbell, Lanni, & Anderson, 2007)

Appendix D – Biodegredation Calculations:

Vo	9.04779E-07	number of layers: 12				
Absolute Density: 1.34g/cm^3 (from Arnold et al. 2007)						
Layer #	Radius	Volume of Layer	Mass of Layer	Deg. Time per layer(days)	Total Deg. Time (days)	secs
1	0.0005	5.23599E-10	0.000701622	44.99981696	161.3226563	1.39E+07
2	0.001	4.18879E-09	0.005612979	26.32320546	116.3228394	1.01E+07
3	0.0015	1.41372E-08	0.018943804	18.6766115	89.99963392	7.78E+06
4	0.002	3.35103E-08	0.044903831	14.48670534	71.32302242	6.16E+06
5	0.0025	6.54498E-08	0.087702795	11.83650012	56.83631708	4.91E+06
6	0.003	1.13097E-07	0.15155043	10.00761825	44.99981696	3.89E+06
7	0.0035	1.79594E-07	0.240656469	8.668993245	34.99219871	3.02E+06
8	0.004	2.68083E-07	0.359230648	7.646593962	26.32320546	2.27E+06
9	0.0045	3.81704E-07	0.5114827	6.840111382	18.6766115	1.61E+06
10	0.005	5.23599E-07	0.701622359	6.1876334	11.83650012	1.02E+06
11	0.0055	6.9691E-07	0.93385936	5.648866716	5.648866716	4.88E+05
12	0.006	9.04779E-07	1.212403437	0	0	0.00E+00
Layer #	Radius	Volume of Layer	Mass of Layer	Degradation Time (days)		
1	0.001	4.18879E-09	0.005612979	44.99981696		
2	0.002	3.35103E-08	0.044903831	26.32320546		
3	0.003	1.13097E-07	0.15155043	18.6766115		
4	0.004	2.68083E-07	0.359230648	14.48670534		
5	0.005	5.23599E-07	0.701622359	11.83650012		
6	0.006	9.04779E-07	1.212403437	0		

Appendix E – Contour Plot

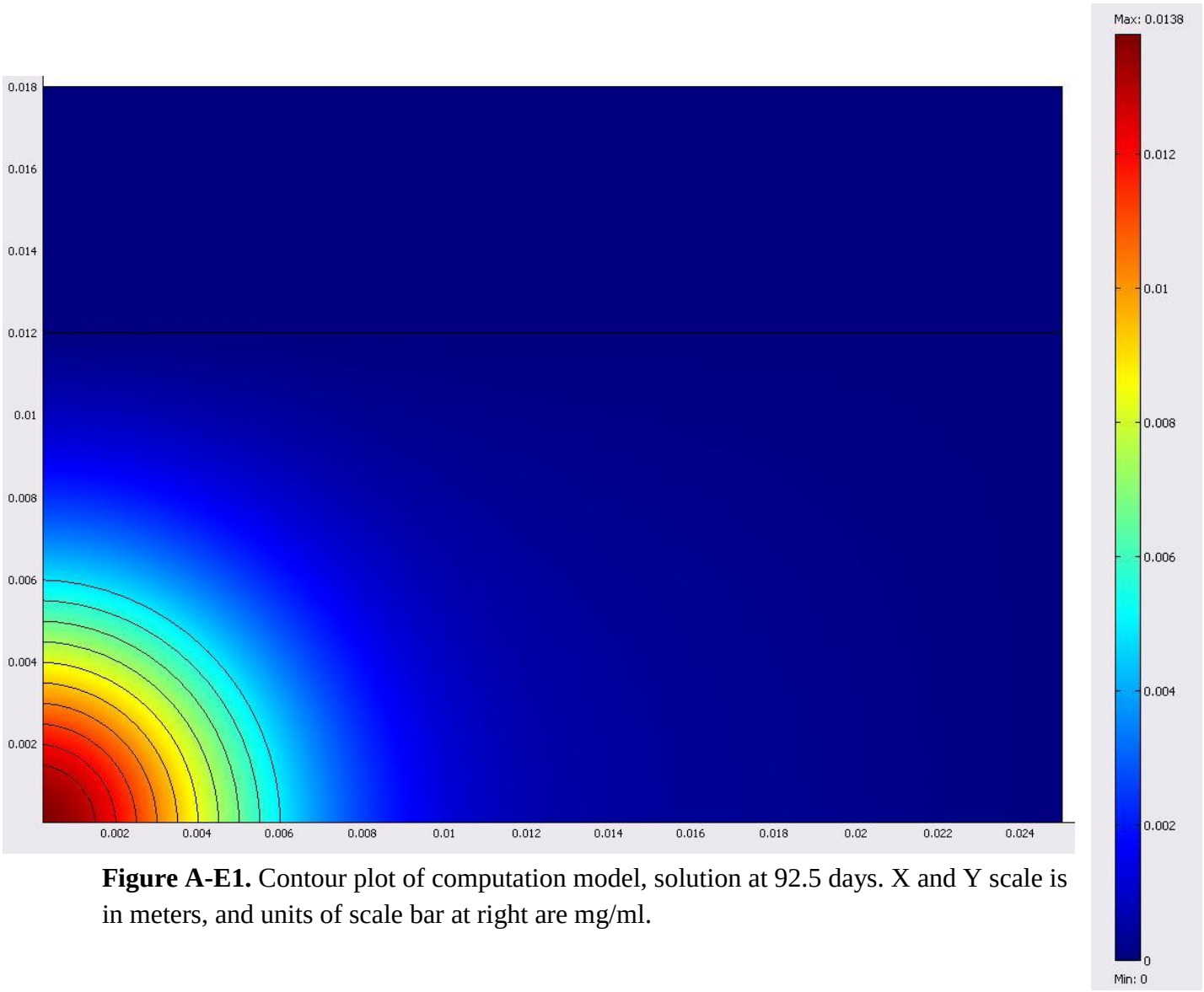

Figure A-E1. Contour plot of computation model, solution at 92.5 days. X and Y scale is in meters, and units of scale bar at right are mg/ml.